Structure of the Bloch wall in multilayers

By Carlos J. García-Cervera

*Mathematics Department, University of California,
Santa Barbara, CA 93106, USA*
(cgarcia@math.ucsb.edu)

We present an analysis of the structure of Bloch walls in layered magnetic materials in the context of micromagnetics. We have obtained the Γ-limit of a one-dimensional reduction of the Landau–Lifshitz energy for a double layer in several asymptotic regimes. As a result, the optimal energy, the core length and the optimal shape of the Bloch wall have been determined. The effects of the interlayer spacing and the film thickness are studied. A comparison between the structure of the Bloch and Néel walls in multilayers is carried out. We illustrate all our findings by numerically minimizing the one-dimensional energy.

Keywords: micromagnetics; Landau–Lifshitz; Γ-limit; Bloch walls; Néel walls

1. Introduction

With the discovery of giant magneto-resistance and interlayer exchange coupling, new applications of layered magnetic structures are being considered, although the magnetic recording industry continues to be the dominating area of interest for these materials (Prinz 1998; Ziese & Thornton 2001; Hirota *et al.* 2002). In layered materials, ideally the magnetic field generated in one of the layers can be balanced by an opposite field generated by the other layer. As a consequence, multilayers have good permanent magnet properties, and in particular, a high coercive field and approximately rectangular hysteresis loop (Puchalska & Niedoba 1991). For that reason, multilayers are an integral part of magnetic memories, and have been one of the most important applications of ferromagnetic thin films in the past few years.

In this article, we analyse the structure of Bloch walls in symmetric double layers consisting of two (infinitely long) ferromagnetic layers of thickness D and width W, separated by a non-magnetic layer of thickness $2a$ (see figure 1). In previous calculations, an a priori functional form for the magnetization with only one or two degrees of freedom is frequently assumed, and the energy is optimized in terms of these free parameters (Middelhoek 1966; Slonczewski 1966a,b). In our work, we do not use an ansatz for the optimal shape of the Bloch wall. We assume that the magnetic layers are coupled only through the stray field, and we use a one-dimensional reduction of the Landau–Lifshitz energy (Landau & Lifshitz 1935; Brown 1963; Aharoni 1996) to analyse the structure of the Bloch wall. The optimal Bloch wall is obtained minimizing this energy functional.
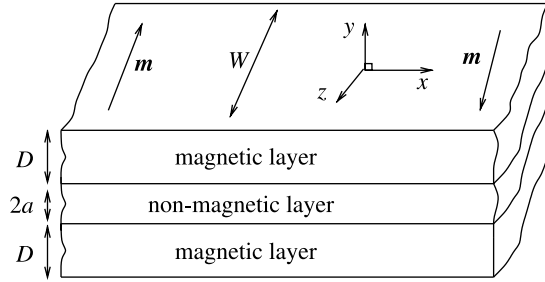
C. J. García-Cervera

Figure 1. One-dimensional wall setting in a multilayer.

In non-dimensional variables, the Landau–Lifshitz energy for a ferromagnetic material occupying a volume V is

$$F[\boldsymbol{m}] = \frac{q}{2} \int_V (u^2 + v^2)\mathrm{d}x + \frac{1}{2} \int_V |\nabla \boldsymbol{m}|^2 \mathrm{d}x - \frac{1}{2} \int_V \boldsymbol{h}_\mathrm{s} \cdot \boldsymbol{m} \, \mathrm{d}x. \qquad (1.1)$$

In equation (1.1) $\boldsymbol{m} = (u, v, w)$ is the magnetization vector, and $|\boldsymbol{m}| = 1$ below the Curie temperature; q is the quality factor and $\boldsymbol{h}_\mathrm{s}$ is the stray field. The quality factor is defined as $q = K_u/(\mu_0 M_\mathrm{s}^2)$, where K_u is the crystalline anisotropy $(\mathrm{J\,m}^{-3})$, μ_0 is the permeability of vacuum $(\mu_0 = 4\pi \times 10^{-7}\,\mathrm{N\,A}^{-2})$, and M_s is the saturation magnetization $(\mathrm{A\,m}^{-1})$. In equation (1.1), lengths are measured in units of the exchange length $l = \sqrt{C_\mathrm{ex}/(\mu_0 M_\mathrm{s}^2)}$, where C_ex is the exchange coupling parameter $(\mathrm{J\,m}^{-1})$. Energy is measured in units of $e = DW\sqrt{\mu_0 M_\mathrm{s}^2 C_\mathrm{ex}}$. The stray field $\boldsymbol{h}_\mathrm{s}$ is obtained by solving the static Maxwell equations in the absence of currents and charges, and it can be evaluated exactly as $\boldsymbol{h}_\mathrm{s} = -\nabla \eta$, where

$$\eta(\boldsymbol{x}) = \frac{1}{4\pi} \int_V \frac{\boldsymbol{x} - \boldsymbol{y}}{|\boldsymbol{x} - \boldsymbol{y}|^3} \cdot \boldsymbol{m}(\boldsymbol{y})\mathrm{d}\boldsymbol{y} \qquad (1.2)$$

is the magnetostatic potential.

Functional (1.1) has a very rich energy landscape, and the structure of the minimizers can be very complex (Choksi & Kohn 1998; Hubert & Schäfer 1998; Choksi *et al.* 1999; De Simone *et al.* 1999, 2003; García-Cervera 1999). It is well known that for thick films, higher dimensional structures such as asymmetric Bloch walls can be observed experimentally (Otto 2002). The aim of this paper is to study the structure and energy scaling of the simpler one-dimensional walls, which can be used as building blocks for more complicated structures.

For the study of one-dimensional walls in single films, Aharoni (1966) introduced the following energy functional, derived from the full Landau–Lifshitz energy under the only assumption that the wall be one-dimensional

$$F_{q,\delta}[\boldsymbol{m}] = \frac{q}{2} \int_\mathbb{R} (u^2 + v^2) + \frac{1}{2} \int_\mathbb{R} |\boldsymbol{m}'|^2 + \frac{1}{2} \int_\mathbb{R} (u^2 - u(\Gamma_\delta * u)) + \frac{1}{2} \int_\mathbb{R} v(\Gamma_\delta u), \quad (1.3)$$

where $\delta = D/l$ represents the (rescaled) thickness of the sample,

$$\Gamma_\delta(x) = \frac{1}{2\pi\delta}\log\left(1 + \frac{\delta^2}{x^2}\right), \qquad (1.4)$$

and the convolution is defined as

$$v * \Gamma_\delta(x) = \int_{-\infty}^{\infty} v(y) \Gamma_\delta(x - y) \mathrm{d}y. \tag{1.5}$$

The set of admissible functions is

$$C = \left\{ \boldsymbol{m} = (u, v, w) \middle| u, v \in H^1(\mathbb{R}), \quad w' \in L^2(\mathbb{R}), \right.$$
$$\left. |\boldsymbol{m}| = 1 \text{ a.e.}, \quad \boldsymbol{m} \to \pm \boldsymbol{e}_3 \text{ as } x \to \pm \infty \right\}. \tag{1.6}$$

Two kinds of one-dimensional structures have been observed experimentally: Néel walls, in which the magnetization rotates in the plane (so $v=0$) and are characteristic of thin films, and Bloch walls, in which the magnetization performs an out-of-plane rotation (so $u=0$), and are characteristic of thick films. The structure of Néel and Bloch walls in single layers has been the subject of much recent work (García-Cervera 1999, 2004; De Simone *et al.* 2003; Melcher 2003, 2004), and a new model for the study of one-dimensional walls in double layers was introduced by García-Cervera (in press). The model was derived from the Landau–Lifshitz energy under the one-dimensional assumption, and a detailed analysis of the Néel wall in multilayers was carried out.

In the Néel wall setting, it was proved that the magnetization rotates in opposite directions in the two layers in order to achieve maximum cancellation in the stray field, which produces an effective anti-ferromagnetic coupling between the layers. As a result, the logarithmic tail, characteristic of the Néel wall in single layers, is no longer present in the double layer case, and the wall becomes more local, with shape similar to that of the Landau–Lifshitz wall (Landau & Lifshitz 1935; García-Cervera in press).

In contrast, we show here that in a multilayer, the Bloch wall rotates in the same direction in both layers, which provides an effective ferromagnetic coupling between the layers. As a consequence, we show that the structure of the Bloch wall in a multilayer is similar to the structure of the Bloch wall in the single layer case.

For the study of Bloch walls ($u_1 = u_2 = 0$), the model derived by García-Cervera (in press) reduces to

$$F_{q,\delta,\alpha}[\boldsymbol{m}_1, \boldsymbol{m}_2] = \frac{q}{2} \int_{\mathbb{R}} v_1^2 \mathrm{d}x + \frac{1}{2} \int_{\mathbb{R}} |\boldsymbol{m}_1'|^2 \mathrm{d}x + \frac{1}{2} \int_{\mathbb{R}} v_1(\Gamma_\delta * v_1) \mathrm{d}x + \frac{q}{2} \int_{\mathbb{R}} v_2^2 \mathrm{d}x$$
$$+ \frac{1}{2} \int_{\mathbb{R}} |\boldsymbol{m}_2'|^2 \mathrm{d}x + \frac{1}{2} \int_{\mathbb{R}} v_2(\Gamma_\delta * v_2) \mathrm{d}x - \frac{\delta}{2} \int_{\mathbb{R}} v_1(\Theta_{\alpha,\delta} * v_2) \mathrm{d}x, \tag{1.7}$$

where $\boldsymbol{m}_1 = (u_1, v_1, w_1)$ and $\boldsymbol{m}_2 = (u_2, v_2, w_2)$ are the magnetization vectors in the top and bottom layer, respectively,

$$\Theta_{\alpha,\delta}(x) = \frac{1}{2\delta^2 \pi} \left(\log\left(\frac{x^2 + (2\alpha + \delta)^2}{x^2 + (2\alpha + 2\delta)^2} \right) - \log\left(\frac{x^2 + 4\alpha^2}{x^2 + (2\alpha + \delta)^2} \right) \right), \tag{1.8}$$

and Γ_δ is as in equation (1.4). In equation (1.8), $\alpha = a/l$ is the rescaled thickness of the non-magnetic interlayer. It is convenient to write the energy in Fourier space, since a convolution in real space becomes multiplication in the frequency domain. The energy (1.7) can be written in Fourier space as

$$F_{q,\delta,\alpha}[\boldsymbol{m}_1, \boldsymbol{m}_2] = \frac{q}{2}\int_{\mathbb{R}}|\widehat{v_1}|^2\mathrm{d}\xi + \frac{1}{2}\int_{\mathbb{R}}|2\pi\xi\widehat{m_1}|^2\mathrm{d}\xi + \frac{1}{2}\int_{\mathbb{R}}|\widehat{v_1}|^2\widehat{\Gamma_\delta}\,\mathrm{d}\xi + \frac{q}{2}\int_{\mathbb{R}}|\widehat{v_2}|^2\mathrm{d}\xi$$

$$+ \frac{1}{2}\int_{\mathbb{R}}|2\pi\xi\widehat{m_2}|^2\mathrm{d}\xi + \frac{1}{2}\int_{\mathbb{R}}|\widehat{v_2}|^2\widehat{\Gamma_\delta}\,\mathrm{d}\xi - \frac{\delta}{2}\int_{\mathbb{R}}\widehat{v_1}\,\overline{\widehat{v_2}}\,\widehat{\Theta_{\alpha,\delta}}\,\mathrm{d}\xi,$$

$$(1.9)$$

where

$$\widehat{\Gamma_\delta}(\xi) = \frac{1 - \mathrm{e}^{-2\pi\delta|\xi|}}{2\pi\delta|\xi|}, \tag{1.10}$$

$$\widehat{\Theta_{\alpha,\delta}}(\xi) = 2\pi|\xi|\mathrm{e}^{-4\pi\alpha|\xi|}\widehat{\Gamma_\delta}^2(\xi) \tag{1.11}$$

Note that both $\widehat{\Gamma_\delta}$ and $\widehat{\Theta_{\alpha,\delta}}$ are positive.

The remainder of this article is organized as follows: a brief summary of the results proved by García-Cervera (in press) regarding the Néel wall are presented in §2. The Bloch wall is considered in §3. We obtain the asymptotic limit of the energy, and a description of the structure of the wall is presented in §4. All these results are illustrated numerically in §5.

2. Néel walls: review

The Néel wall has a very rich structure due to the non-local nature of the interaction in the Landau–Lifshitz energy functional. The optimal energy scaling for a Néel wall in a single layer was obtained by García-Cervera (1999, 2004). It was shown that for a given $\delta > 0$, positive constants c_0 and C_0 exist, such that

$$\frac{c_0}{\log(1/q)} \le \inf_{\boldsymbol{m}\in\mathcal{C}, m_2=0} F_{q,\delta}[\boldsymbol{m}] \le \frac{C_0}{\log(1/q)}, \tag{2.1}$$

where $\mathcal{C}$ is defined in equation (1.6).

It was also shown that the Néel wall has a long, logarithmic tail, which extends the stray field interaction to great distances. An improvement of this result, with higher order terms in the energy scaling was used by De Simote et al. (1999), and some new results in this direction have appeared in the work of Melcher (2003, 2004).

The interactions between Néel walls in a double layer were considered by García-Cervera (in press). It was shown that the stray field induces an anti-ferromagnetic coupling between the layers that maximizes the cancellations in the stray field. As a result, the optimal energy changes dramatically, and it was

shown that

$$4\sqrt{q} \le \inf_{\boldsymbol{m}\in\mathcal{C},\, m_2=0} F_{q,\alpha,\delta}[\boldsymbol{m}] \le C_0\sqrt{q} \tag{2.2}$$

for some positive constant C_0. The Néel wall in a symmetric double layer no longer has a logarithmic tail. The internal length scale of the transition layer is of order $O(q^{-1/2})$, and the limiting profile of the wall (as $q\to 0$) is the minimizer of

$$G_{\alpha,\delta}[\boldsymbol{m}] = \int_{\mathbb{R}} m_1^2 \, \mathrm{d}x + \frac{\delta(\delta+3\alpha)}{3} \int_{\mathbb{R}} (m_1')^2 \, \mathrm{d}x + \int_{\mathbb{R}} |m'|^2 \mathrm{d}x. \tag{2.3}$$

3. Ferromagnetic coupling and asymptotic limits

The magnetization in a Bloch wall undergoes an out-of-plane rotation, as opposed to the Néel walls, where the rotation is in-plane. As a result the structure of the Bloch wall, described in theorem 3.2 below, is very different from that of the Néel wall. In a double layer, one of the consequences of this out-of-plane rotation is that the Bloch wall that appears in one layer is effectively ferromagnetically coupled to the Bloch wall in the other layer, as shown in lemma 3.1 below. This ferromagnetic coupling prevents certain cancellations in the stray field from occurring, and therefore the differences in the structure of the Bloch wall between a single and a double layer are not as dramatic as in the Néel wall case, described in §2.

Lemma 3.1. *If* $(\boldsymbol{m}_1, \boldsymbol{m}_2)$ *is a global minimizer of* (1.7), *where* $\boldsymbol{m}_1 = (0, v_1, w_1)$ *and* $\boldsymbol{m}_2 = (0, v_2, w_2)$, *then* $v_1 = v_2$.

Proof. The existence of minimizers can be established following the same proof as in the Néel wall case (see García-Cervera in press; lemma 2.1 and the subsequent discussion), and will not be presented here.

The energy functional (1.7) can be rewritten as

$$\begin{aligned} F_{q,\delta,\alpha}[\boldsymbol{m}_1, \boldsymbol{m}_2] &= \frac{1}{2} F_{q,\delta,\alpha}[\boldsymbol{m}_1, \boldsymbol{m}_1] + \frac{1}{2} F_{q,\delta,\alpha}[\boldsymbol{m}_2, \boldsymbol{m}_2] \\ &\quad + \frac{\delta}{4} \int_{\mathbb{R}} (v_1 - v_2)\cdot\boldsymbol{\Theta}_{\alpha,\delta}*(v_1 - v_2) \, \mathrm{d}x. \end{aligned} \tag{3.1}$$

Each term in the previous expression is non-negative, and therefore for the minimum energy we need $v_1 = v_2$, effectively producing a ferromagnetic coupling between the layers. ∎

As a consequence of lemma 3.1, we only need to study the energy functional

$$F_{q,\delta,\alpha}[\boldsymbol{m}] = q \int_{\mathbb{R}} v^2 \, \mathrm{d}x + \int_{\mathbb{R}} |\boldsymbol{m}'|^2 \mathrm{d}x + \int_{\mathbb{R}} v\left(\Gamma_\delta - \frac{\delta}{2}\Theta_{\alpha,\delta}\right)*v \, \mathrm{d}x, \tag{3.2}$$

or in Fourier space

$$F_{q,\delta,\alpha}[\boldsymbol{m}] = q \int_{\mathbb{R}} |\widehat{v}|^2 \mathrm{d}\xi + \int_{\mathbb{R}} |2\pi\xi\widehat{m}|^2 \mathrm{d}\xi + \int_{\mathbb{R}} |\widehat{v}|^2 \left(\widehat{\Gamma_\delta} - \frac{\delta}{2}\widehat{\Theta_{\alpha,\delta}}\right) \mathrm{d}\xi. \tag{3.3}$$

We proceed now to study the energy functional (3.3) and the effects of the interlayer spacing, and the thickness of the ferromagnetic layers.

For $\alpha = 0$, note that

$$\left(\widehat{\Gamma_\delta} - \frac{\delta}{2}\widehat{\Theta_{0,\delta}}\right)(\xi) = \widehat{\Gamma_\delta}(\xi)(1 - \pi\delta|\xi|\widehat{\Gamma_\delta}(\xi)) = \frac{(1 - e^{-2\pi\delta|\xi|})(1 + e^{-2\pi\delta|\xi|})}{4\pi\delta|\xi|} = \widehat{\Gamma_{2\delta}}(\xi), \tag{3.4}$$

and the energy functional (1.7) reduces to Aharoni's model (1.3) for a Bloch wall. Therefore, when $\alpha \ll 1$, the minimum energy in the double layer is obtained by the Bloch wall that corresponds to a single layer of thickness 2δ, in agreement with the experiments and observations done by Middelhoek (1966).

If $\alpha \gg 1$, and $\delta = O(1)$, the interaction between the two layers vanishes, and we obtain a Bloch wall in each layer of thickness δ.

Before we proceed with the rigorous analysis of functional (3.2), we give a heuristic argument to determine the relevant length-scales, energy scaling and asymptotic regimes.

If $\delta \gg 1$, the leading term in the energy is of the form

$$F_{q,\delta,\alpha}[\boldsymbol{m}] \sim q\int_{\mathbb{R}} v^2 + \int_{\mathbb{R}} |\boldsymbol{m}'|^2 + \frac{1}{\delta}\int_{\mathbb{R}} \frac{|\widehat{v}|^2}{|\xi|}\,\mathrm{d}\xi. \tag{3.5}$$

In order to determine the optimal wall length, we look for a wall profile of the form $\boldsymbol{m}(x) = \boldsymbol{m}(\lambda x)$, and optimize in λ. In terms of λ, the energy scales like

$$E \sim \frac{q}{\lambda} + \lambda + \frac{1}{\delta\lambda^2}. \tag{3.6}$$

Optimizing in λ, we need to solve the following equation:

$$\lambda^3 - q\lambda - \frac{2}{\delta} = 0. \tag{3.7}$$

For parameters typical of permalloy ($C_{\mathrm{ex}} = 1.3 \times 10^{-11}$ J m^{-1}, $K_u = 5 \times 10^2$ J m^{-3}, $M_s = 8 \times 10^5$ A m^{-1}), the quality factor is $q \approx 6.21 \times 10^{-3}$, so we are interested in the low anisotropy limit. If $q = 0$, then $\lambda = O(\delta^{-1/3})$, which motivates the change of variable $\lambda = \delta^{-1/3}\mu$. Equation (3.7) becomes

$$\mu^3 - q\delta^{2/3}\mu - 2 = 0. \tag{3.8}$$

Since we are mostly interested in the effect that the stray field has in the structure of the wall, we only consider here the asymptotic regimes $q\delta^{2/3} = O(1)$ and $q\delta^{2/3} \ll 1$, which both yield $\mu = O(1)$, or $\lambda = O(\delta^{-1/3})$. Consequently, $E \sim \delta^{-1/3}$ in this regime. This heuristic argument suggests the change of variable $x \to \delta^{1/3}y$, and the energy rescaling: $\tilde{F}_{q,\alpha,\delta} = \delta^{1/3}F_{q,\alpha,\delta}$.

If $\tilde{\boldsymbol{m}}_\delta(x) = \boldsymbol{m}(\delta^{-1/3}x)$, then

$$\widehat{\tilde{\boldsymbol{m}}_\delta}(\xi) = \delta^{1/3}\widehat{\boldsymbol{m}}(\delta^{1/3}\xi). \tag{3.9}$$

Therefore, the energy becomes

$$\tilde{F}_{q,\delta,\alpha}[\boldsymbol{m}] = q\delta^{2/3}\int_{\mathbb{R}} v^2 + \int_{\mathbb{R}} |\boldsymbol{m}'|^2 \mathrm{d}x$$

$$+ \int_{\mathbb{R}} |\widehat{v}|^2(\xi)\left(\frac{1-\mathrm{e}^{-2\pi\delta^{2/3}|\xi|}}{2\pi|\xi|} - \mathrm{e}^{-4\pi\alpha\delta^{-1/3}}|\xi|\frac{(1-\mathrm{e}^{-2\pi\delta^{2/3}|\xi|})^2}{4\pi|\xi|}\right)\mathrm{d}\xi, \quad (3.10)$$

and we observe three additional distinguished limits: $\alpha \ll \delta^{1/3}$, $\alpha \gg \delta^{1/3}$ and $\alpha \sim \delta^{1/3}$. We proceed to analyse each situation. A natural setting for the study of the limiting behaviour of the minimizers of a family of functionals is the notion of Γ-convergence (Dal Maso 1993), by which we identify the limits as minimizers of a certain limit functional. For our purposes, we only need the following characterization of Γ-convergence (Dal Maso 1993), which is often taken as its definition:

Theorem 3.1. *Let* $(X, \mathcal{T})$ *be a topological space, and let* F_h *be a family of functionals parametrized by h. A functional* F_0 *is the Γ-limit of* F_h *as* $h \to 0$ *in* $\mathcal{T}$*, if and only if the two following conditions are satisfied:*

(i) *If* $u_h \to u_0$ *in* $\mathcal{T}$*, then* $\liminf_{h\to 0} F_h(u_h) \geq F_0(u_0)$*.*
(ii) *For all* $u_0 \in X$*, there exists a sequence* $u_h \in X$*, such that* $u_h \to u_0$ *in* $\mathcal{T}$*, and* $\lim_{h\to 0} F_h(u_h) = F_0(u_0)$*.*

In the following theorem, we identify the Γ-limit of (3.10) in the different asymptotic regimes.

Theorem 3.2. *Consider functional* (3.10), *defined in*

$$\mathcal{A} = \{\boldsymbol{m} = (0, v, w) : \mathbb{R} \to \mathbb{R}^3 \,\big|\, |\boldsymbol{m}| = 1, \quad v \in H^1(\mathbb{R}), \quad w' \in L^2(\mathbb{R})\}. \quad (3.11)$$

Assume that $\delta \to \infty$ *and* $q \to 0$ *in such a way that* $q\delta^{2/3} \to \gamma \geq 0$*. Consider*

$$\mathcal{B} = \{\boldsymbol{m} = (0, v, w) : \mathbb{R} \to \mathbb{R}^3 \,\big|\, |\boldsymbol{m}| = 1, \quad v \in H^{-1/2}(\mathbb{R}), \quad \boldsymbol{m}' \in L^2(\mathbb{R})\}. \quad (3.12)$$

For $\boldsymbol{m} \in \mathcal{A}$*, define*

$$F_{0,\gamma}[\boldsymbol{m}] = \begin{cases} \gamma\int_{\mathbb{R}} v^2\,\mathrm{d}x + \int_{\mathbb{R}} |\boldsymbol{m}'|^2\mathrm{d}x + \dfrac{1}{4\pi}|v|^2_{H^{-1/2}(\mathbb{R})}, & \boldsymbol{m} \in \mathcal{B}, \\ +\infty, & \text{otherwise,} \end{cases} \quad (3.13)$$

$$F_{1,\gamma}[\boldsymbol{m}] = \begin{cases} \gamma\int_{\mathbb{R}} v^2\,\mathrm{d}x + \int_{\mathbb{R}} |\boldsymbol{m}'|^2\mathrm{d}x + \dfrac{1}{2\pi}|v|^2_{H^{-1/2}(\mathbb{R})}, & \boldsymbol{m} \in \mathcal{B}, \\ +\infty, & \text{otherwise,} \end{cases} \quad (3.14)$$

where

$$|v|^2_{H^{-1/2}(\mathbb{R})} = \int_{\mathbb{R}} \frac{|\widehat{v}|^2}{|\xi|}\,\mathrm{d}\xi, \quad (3.15)$$

and

$$F_{2,\gamma,\beta}[\boldsymbol{m}] = \begin{cases} \gamma \displaystyle\int_{\mathbb{R}} v^2 \, \mathrm{d}x + \int_{\mathbb{R}} |\boldsymbol{m}'|^2 \mathrm{d}x + \int_{\mathbb{R}} |\widehat{v}|^2 \left(\dfrac{1}{4\pi|\xi|} + \beta \widehat{\Gamma}_{2\beta}(\xi) \right) \mathrm{d}\xi, & \boldsymbol{m} \in \mathcal{B}, \\[3mm] +\infty, & \text{otherwise.} \end{cases}$$
$$(3.16)$$

Then, the following hold.

(i) *If $\alpha \ll \delta^{1/3}$,*

$$\Gamma - \lim_{\delta \to \infty} \tilde{F}_{q,\delta,\alpha}[\boldsymbol{m}] = F_{0,\gamma}[\boldsymbol{m}]. \tag{3.17}$$

(ii) *If $\alpha \gg \delta^{1/3}$,*

$$\Gamma - \lim_{\delta \to \infty} \tilde{F}_{q,\delta,\alpha}[\boldsymbol{m}] = F_{1,\gamma}[\boldsymbol{m}]. \tag{3.18}$$

(iii) *If $\alpha = \beta \delta^{1/3}$,*

$$\Gamma - \lim_{\delta \to \infty} \tilde{F}_{q,\delta,\alpha}[\boldsymbol{m}] = F_{2,\gamma,\beta}[\boldsymbol{m}]. \tag{3.19}$$

Proof. We only include the proof of (i), since the others are similar. To establish the Γ-limit in (i), we need to show that the two conditions in theorem 3.1 are met.

To prove condition (i) in theorem 3.1, we consider a sequence $\{\boldsymbol{m}_\delta\}$ such that

$$\tilde{F}_{q,\alpha,\delta}[\boldsymbol{m}_\delta] \le M, \quad \forall \, \delta > 0, \tag{3.20}$$

for some $M > 0$. Since the energy is translation invariant, we can assume that $\boldsymbol{m}_\delta(0) = \boldsymbol{e}_2$ for all $\delta > 0$. It follows from lemma 3.2 below that the sequence is uniformly bounded in $H^1(\mathbb{R})$. Therefore, there exists a subsequence (not relabelled) which will converge to some $\boldsymbol{m} \in \mathcal{A}$ weakly in $H^1(\mathbb{R})$ and strongly in $L^2_{\mathrm{loc}}(\mathbb{R})$.

Give $\epsilon > 0$, $\exists \delta_0 > 0$ such that $\forall \delta \ge \delta_0$ and $\forall |\xi| \ge \delta^{-2/3}$:

$$\left(\frac{1 - \mathrm{e}^{-2\pi\delta^{2/3}|\xi|}}{2\pi} - \mathrm{e}^{-4\pi\alpha\delta^{-1/3}|\xi|} \frac{(1 - \mathrm{e}^{-2\pi\delta^{2/3}|\xi|})^2}{4\pi} \right) \ge \frac{1}{4\pi} - \epsilon. \tag{3.21}$$

Therefore, $\exists C > 0$ such that

$$\int_{|\xi| \ge \delta^{-2/3}} \frac{|\widehat{v}\delta|^2}{|\xi|} \, \mathrm{d}\xi \le C, \quad \forall \, \delta > 0. \tag{3.22}$$

As a consequence, $\boldsymbol{m} \in \mathcal{B}$, and (i) follows from the weak convergence of the sequence $\{\boldsymbol{m}_\delta\}$ in H^1, and lemma 3.3 below.

To prove (ii) in theorem 3.1, given $\boldsymbol{m} \in \mathcal{B}$, consider $\boldsymbol{m}_\delta = \boldsymbol{m}$ for all $\delta > 0$. The result follows from the dominated convergence theorem. ∎

The proof of theorem 3.2 relies on lemmas 3.2 and 3.3 below. In lemma 3.2 we establish a kind of interpolation inequality. If follows from this lemma that a sequence of functions for which functional 3.10 is bounded will be uniformly bounded in $H^1(\mathbb{R})$.

Lemma 3.2. *Consider* $\Sigma_{\alpha,\delta} = \Gamma_\delta - \delta/2\Theta_{\alpha,\delta}$. *There exists an* $\epsilon_0 > 0$ *such that* $\forall 0 < \epsilon \leq \epsilon_0$

$$\int_{\mathbb{R}} v^2 \, \mathrm{d}x \leq \frac{1}{\widehat{\Sigma_{\alpha,\delta}}(\varepsilon)} \int_{\mathbb{R}} v(\Sigma_{\alpha,\delta} * v) \mathrm{d}x + \frac{1}{4\pi^2 \varepsilon^2} \int_{\mathbb{R}} (v')^2 \mathrm{d}x. \tag{3.23}$$

Proof. Using Plancherel's theorem, and since $\widehat{\Sigma_{\alpha,\delta}}(\xi)$ is a decreasing function of ξ in $|\xi| \in [0, \epsilon_0]$ for some $\epsilon_0 > 0$, we obtain

$$\begin{aligned}
\int_{\mathbb{R}} v^2 \, \mathrm{d}x &= \int_{|\xi| \leq \varepsilon} \widehat{v}^2 \, \mathrm{d}\xi + \int_{|\xi| > \varepsilon} \widehat{v}^2 \, \mathrm{d}\xi \\
&\leq \frac{1}{\widehat{\Sigma_{\alpha,\delta}}(\varepsilon)} \int_{|\xi| \leq \varepsilon} \widehat{v}^2 \widehat{\Sigma_{\alpha,\delta}}(\xi) \mathrm{d}\xi + \frac{1}{\varepsilon^2} \int_{|\xi| \leq \varepsilon} \xi^2 \widehat{v}^2 \, \mathrm{d}\xi,
\end{aligned} \tag{3.24}$$

which gives the desired inequality. ∎

In the following lemma, proved by García-Cervera (2004), we establish the weak convergence of the non-local term in equation (3.10). The lower semi-continuity of the family of functionals $\{\tilde{F}_{\alpha,\delta}\}_{\delta > 0}$ with respect to weak convergence in $\mathcal{B}$ follows directly from it.

Lemma 3.3. *Consider a family of functions* $\{K_h\}_{h>0} \subset L^1(\mathbb{R}^n) \cap L^2(\mathbb{R}^n)$ *such that the family of Fourier transformers* $\{\widehat{K}_h\}_{h>0} \subset L^\infty(\mathbb{R}^n) \cap L^2(\mathbb{R}^n)$ *is uniformly bounded. Assume that*

$$\lim_{h \to 0} \widehat{K}_h(\xi) = \widehat{K}_0(\xi) \quad \text{for almost all } \xi \in \mathbb{R}^n, \tag{3.25}$$

where $\widehat{K}_0 \in L^\infty(\mathbb{R}^n)$. *Then, if* $\{u_h\}_{h>0} \subset L^2(\mathbb{R}^n)$ *converges weakly in* $L^2(\mathbb{R}^2)$ *to* $u_0 \in L^2(\mathbb{R}^n)$ *as* $h \to 0$, *then the family* $\{v_h\}_{h>0} = \{u_h K_h\}_{h>0}$ *converges weakly in* $L^2(\mathcal{R}^n)$ *to* $v_0 = \mathcal{F}^{-1}(\widehat{u}_0 \widehat{K}_0)$, *where we denote by* $\mathcal{F}^{-1}$ *the inverse Fourier transform.*

4. Structure of the Bloch wall

In order to understand the structure of the minimizers of energy functional

$$F[\boldsymbol{m}] = \int_{\mathbb{R}} |\boldsymbol{m}'|^2 + \frac{1}{4\pi} \int_{\mathbb{R}} \frac{|\widehat{v}|^2}{|\xi|} \mathrm{d}\xi, \tag{4.1}$$

we use an exact Fourier representation of the minimizer of a related energy functional, following the methodology introduced by García-Cervera (1999, 2004). We compare the structure obtained in this section with the numerically computed minimizer of equation (4.1) in §5.

For the numerical simulations presented in §5, we write functional (4.1) in real space as

$$F[\boldsymbol{m}] = \int_{\mathbb{R}} |\boldsymbol{m}'|^2 \mathrm{d}x + \int_{\mathbb{R}} (v * \varphi)^2 \mathrm{d}\xi \qquad (4.2)$$

where $\widehat{\varphi}(\xi) = 1/\sqrt{4\pi|\xi|}$. Inverting this Fourier transform, we obtain

$$\varphi(x) = \frac{1}{\sqrt{4\pi}} \int_{\mathbb{R}} e^{2\pi i \xi x} \frac{1}{\sqrt{|\xi|}} \mathrm{d}\xi = \frac{2}{\sqrt{4\pi}} \int_0^\infty \frac{\cos(2\pi\xi x)}{\sqrt{\xi}} \mathrm{d}\xi = \frac{1}{2\pi}\sqrt{\frac{\pi}{|x|}}. \qquad (4.3)$$

Since $|\boldsymbol{m}| = 1$, we can write $\boldsymbol{m} = (0, g, \pm\sqrt{1-g^2})$, and the energy (4.1) becomes

$$F[g] = \int_{\mathbb{R}} \frac{(g')^2}{1-g^2} \mathrm{d}x + \frac{1}{4\pi} \int_{\mathbb{R}} \frac{|\widehat{g}|^2}{|\xi|} \mathrm{d}\xi. \qquad (4.4)$$

The nonlinearity is seen only in the exchange term, and the main contribution will be near $x=0$, since $g(0)=1$. Thus, we can get a qualitative description of the minimizer by replacing this functional by

$$G[g] = \int_{\mathbb{R}} (g')^2 \mathrm{d}x + \frac{1}{4\pi} \int_{\mathbb{R}} \frac{|\widehat{g}|^2}{|\xi|} \mathrm{d}\xi, \qquad (4.5)$$

and minimizing it with the constraint that $g(0)=1$. Since $|g| \leq 1$, this procedure always provides us with a lower bound on the energy (4.4). The advantage of this procedure is that we can then solve the minimization problem for (4.4) exactly in Fourier space. The minimizer is

$$\widehat{g}(\xi) = \frac{1}{2} \frac{C_0}{4\pi^2|\xi|^2 + \frac{1}{4\pi|\xi|}}, \qquad (4.6)$$

where C_0 is chosen so that $g(0)=1$. From

$$1 = g(0) = \int_{\mathbb{R}} \widehat{g}(\xi) \mathrm{d}\xi = \int_{\mathbb{R}} \frac{C_0}{4\pi^2|\xi|^2 + \frac{1}{4\pi|\xi|}} \mathrm{d}\xi, \qquad (4.7)$$

we obtain $C_0 = 3(3^{1/2})4^{1/3}/2 \approx 4.124\,188\,910\,995\,81$. Then

$$g(x) = C_0 \int_0^\infty \cos(2\pi\xi x) \frac{4\pi\xi}{1 + 16\pi^3\xi^3} \mathrm{d}\xi. \qquad (4.8)$$

We can rewrite this using residues as

$$g(x) = \frac{C_0}{3 \cdot 2^{2/3}} \exp\left\{-\frac{\sqrt{3}}{2^{4/3}}|x|\right\} \left(\sqrt{3}\cos\left(\frac{|x|}{2^{4/3}}\right) - \sin\left(\frac{|x|}{2^{4/3}}\right)\right)$$
$$- \frac{C_0}{\pi} \int_0^\infty e^{-t|x|} \frac{t}{1 + 4t^6} \mathrm{d}t. \qquad (4.9)$$

This expression shows the presence of oscillations near the core of the Bloch wall, and fast decay in the tail. The presence of these oscillations is necessary so that the total magnetization is zero. The energy of this profile can be computed by

evaluating equation (4.5)

$$G[g] = \int_{\mathbb{R}} |\widehat{g}|^2 \left(4\pi^2\xi^2 + \frac{1}{4\pi|\xi|}\right)\mathrm{d}\xi = C_0. \tag{4.10}$$

Taking into account the energy rescaling considered, we expect the Bloch wall energy to be $E \sim C_0 \delta^{-1/3}$.

A similar approximation to the one presented here can be performed for the other functionals in theorem 3.2. However, since the leading term in the stray field energy in equation (3.16) is the same as in equation (3.13), we obtain the same qualitative behaviour, and therefore the analysis will be omitted here.

5. Numerical experiments

We have developed a modified Newton's method with an inexact line search for energy minimization (Dennis & Schnabel 1983; Nocedal & Wright 1999). The method is well known, so we will only describe our implementation briefly.

We consider a finite interval $I = [-M, M]$, and restrict the functional to I. We have performed simulations in several intervals of increasing size until no change was found in the characteristics of the wall. For the results presented here, we used $I = [-200, 200]$, although in the figures a smaller interval is shown for clarity of presentation. We define the grid points $x_i = -M + i\Delta x$, for $i = 0, 1, \ldots, n+1$, where $\Delta x = 2M/(n+1)$. The magnetization is approximated using linear interpolation in the subinterval $I_i = [x_i, x_{i+1}]$, for $i = 0, 1, \ldots, n$. We impose the boundary conditions $u_0 = u_{n+1} = 0$. The parameter δ was varied in the range $\delta \in [1, 1024]$. The value of the parameter α did not seem to produce any significant change, except in the regime $\alpha \sim \delta^{1/3}$. For the simulations shown here we set $\alpha = 1$.

To evaluate the stray field, we need to approximate convolution integrals of the form

$$v(x_j) = \int_{-M}^{M} u(s)K(x_j - s)\mathrm{d}s. \tag{5.1}$$

Substituting the piecewise linear interpolant for u, and grouping terms, we can write the convolution in the form

$$v_j = \sum_{i=1}^{n} K_{j-i}u_i, \tag{5.2}$$

where

$$K_\lambda = \Delta x \int_0^1 (1-t)K(\Delta x(\lambda - t)) + tK(\Delta x(\lambda + 1 - t)\mathrm{d}t. \tag{5.3}$$

The sum (5.2) has the shape of a discrete convolution, and it can therefore be efficiently evaluated using the fast Fourier transform in $O(n \log n)$ operations. The integrals in equation (5.3) can be evaluated to machine precision using adaptive Gaussian quadrature (Isaacson & Keller 1966).
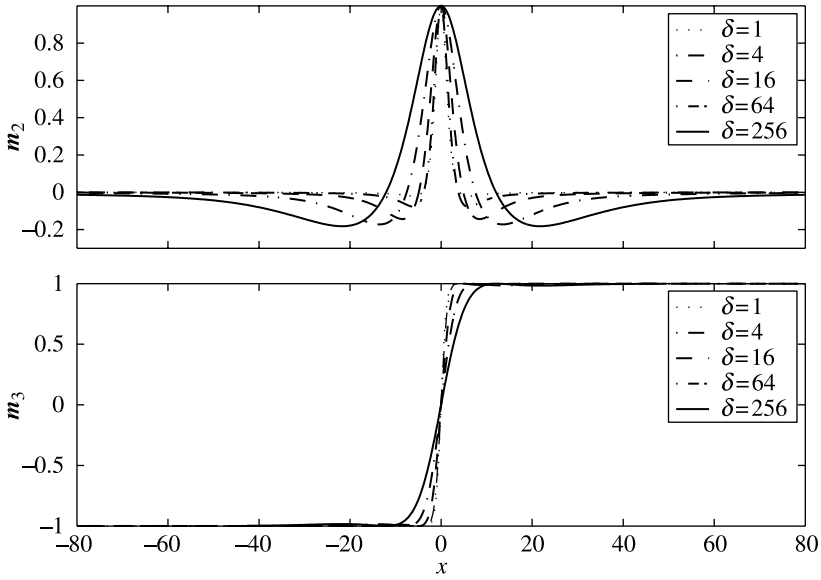
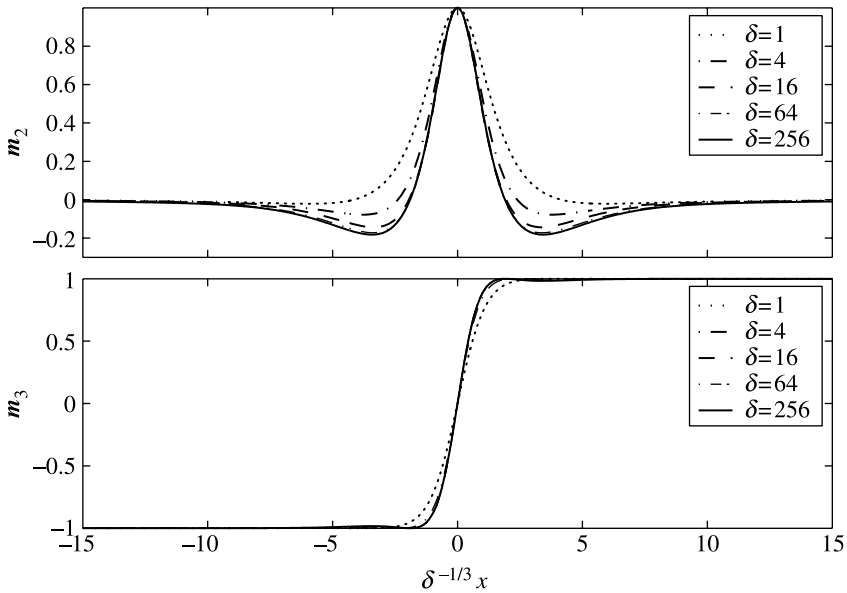Figure 2. Bloch wall structure as a function of δ, for $\alpha=1$.

Figure 3. Bloch wall structure as a function of δ, with OX-axis rescaled, for $\alpha=1$. The shape of the wall converges to a limiting profile.

The unit length constraint in the magnetization is taken into account by considering a line search on the function

$$h(\epsilon) = F_{q,\alpha,\delta}\left[\frac{\boldsymbol{m} + \epsilon\boldsymbol{p}}{|\boldsymbol{m} + \epsilon\boldsymbol{p}|}\right],$$

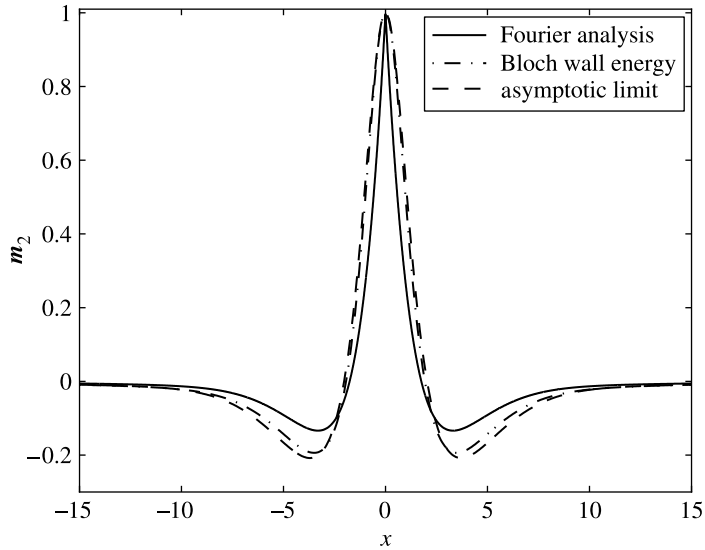where $\boldsymbol{p}$ is a descent direction, i.e. $h'(0)<0$.

Figure 4. The Bloch wall profile for $\delta = 256$ and $\alpha = 1$, obtained minimizing the Bloch wall energy (1.7), is compared with the minimizer of the limiting energy (4.1), and the profile obtained using Fourier analysis (4.9).
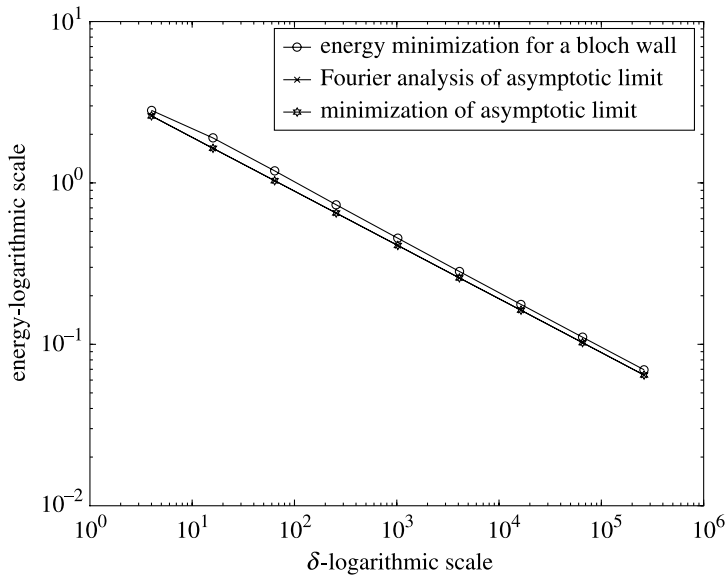

Figure 5. Log–log plot of the energy as a function of δ for $\alpha = 1$. We plot the minimum energy of (1.7) for different values of δ, and compare it with the limiting energy (4.1) and the energy of the Fourier approximation (4.9).

We have used this method to obtain both the minimum energy and the structure of the optimal wall profile for functionals (1.7), (4.1), (4.5) and (3.19).

In figure 2 we show the structure of the Bloch wall for several values of the parameter δ. We can see the oscillations predicted by the Fourier representation
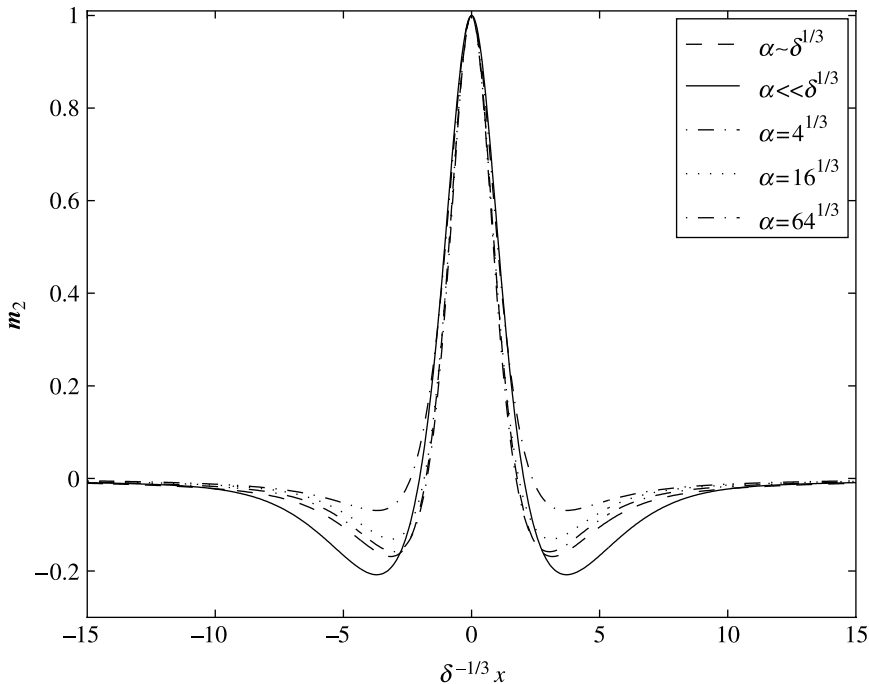
Figure 6. Bloch wall profiles in the regime $\alpha = \delta^{1/3}$, $\delta \gg 1$. Convergence to the minimizer of energy (3.19) is apparent. The profiles are compared with the minimizer in the regime $\alpha = \delta^{1/3}$ to show the qualitative similarities.

(4.9), which do not appear in the classical Landau–Lifshitz wall (Landau & Lifshitz 1935).

The same wall profiles are shown again in figure 3, but the *OX*-axis has been rescaled by $\delta^{-1/3}$. It is clearly seen that the wall profiles converge as $\delta \to \infty$, confirming that the core length of the wall is $\delta^{1/3}$.

In figure 4, we plot the representation (4.9), and compare it to the minimizers of (1.7) and (4.1). The profile obtained using the Fourier approximation described earlier gives a very good qualitative description of the actual minimizer. It is also clear that the energy (4.1) accurately captures the asymptotic behaviour of equation (1.7) as $\delta \to \infty$.

We present in figure 5 the energy obtained by minimizing (1.7) and (4.1). In addition, we have included the energy of the Fourier approximation:

$$E = C_0 \frac{1}{\delta^{1/3}}. \tag{5.5}$$

The minimizer for the asymptotic energy (4.1), computed numerically, is $C_1 = 4.129\,787\,529\,753\,19$. Energy (4.1) predicts a Bloch wall energy $E \sim C_1 \delta^{-1/3}$, in very good agreement with the energy obtained using the Fourier approximation. It follows from figure 5 that we have captured the right energy scaling. In addition, the energy obtained from the Fourier representation is indistinguishable from the energy obtained minimizing (4.1).

Finally, in figure 6, we plot the minimizers of energy (1.7) for several values of δ, and for $\alpha = \delta^{1/3}$. These profiles are compared with the minimizer of the limiting energy (3.19) with $\beta = 1$, showing good agreement. The minimizer of (4.1) is also plotted for comparison. The qualitative details of the walls are the same, but there are some small quantitative differences.

6. Conclusions

We have used a new one-dimensional model to analyse the structure and energy of the Bloch wall in symmetric double layers. We have shown that the Bloch wall energy induces an effective ferromagnetic coupling between the layers, as opposed to the Néel wall case, where the coupling is anti-ferromagnetic. As a result, the structure of the Bloch wall in double layers is very similar to the structure of the same wall in single layers, in contrast to the Néel wall case, where significant structural changes have been reported (García-Cervera in press).

In physical variables, the Bloch wall was found to have a core length

$$\text{core length} \sim D^{1/3}(\mu_0 M_s^2)^{-1/3} C_{\text{ex}}^{1/3}, \qquad (6.1)$$

and optimal energy

$$\text{Bloch wall energy} \sim D^{2/3} W C_{\text{ex}}^{2/3} (\mu_0 M_s^2)^{1/3}. \qquad (6.2)$$

The interplay between the crystalline anisotropy, film thickness, and interlayer spacing has been analysed, and the structure of the Bloch wall has been determined for the corresponding asymptotic regimes in the context of Γ-convergence.

Using Fourier analysis and a convexification of the Landau–Lifshitz energy we have obtained a good qualitative description of the limiting profile of the Bloch wall. The numerical results presented show very good agreement between the structure and energy of this exact minimizer and the numerically computed Bloch walls.

The minimizers of the Landau–Lifshitz energy functional can be very complex, and Bloch walls can be used as building blocks of these more complicated patterns. With the analysis of the Bloch and Néel walls, we have laid down the foundation for the study of higher dimensional structures such as cross-tie walls and asymmetric Bloch walls in multilayers.

References

Aharoni, A. 1966 Energy of one dimensional domain walls in ferromagnetic films. *J. Appl. Phys.* **37**, 3271–3279.

Aharoni, A. 1996 *Introduction to the theory of ferromagnetism.* International series of monographs on physics. Oxford: Oxford University Press.

Brown Jr, W. F. 1963 *Micromagnetics.* Interscience tracts on physics and astronomy. New York/London: Interscience Publishers/Wiley.

Choksi, R. & Kohn, R. V. 1998 Bounds on the micromagnetic energy of a uniaxial ferromagnet. *Commun. Pure Appl. Math.* **51**, 259–289.

Choksi, R., Kohn, R. V. & Otto, F. 1999 Domain branching in uniaxial ferromagnets: a scaling law for the minimum energy. *Commun. Math. Phys.* **201**, 61–79.

Dal Maso, G. 1993 *Introduction to Γ-convergence. Progress in nonlinear differential equations and their applications.* Boston, MA: Birkhauser.

De Simone, A., Kohn, R. V., Müller, S. & Otto, F. 1999 In Magnetic microstructures—a paradigm of multiscale problems. In *ICIAM 99 Proceeding of the Fourth International Congress on Industrial & Applied Mathematics, Edinburgh* (ed. J. M. Ball & J. C. R. Hunt), pp. 175–190. Oxford: Oxford University Press.

De Simone, A., Kohn, R. V., Müller, S. & Otto, F. 2003 Repulsive interaction of Néel walls, and the internal length scale of the cross-tie wall. *Multiscale Model. Simul.* **1**, 57–104.

Dennis Jr, J. E. & Schnabel, R. B. 1983 *Numerical methods for unconstrained optimization and nonlinear equations.* Series in computational mathematics. Englewood Cliffs, NJ: Prentice-Hall.

García-Cervera, C. J. 1999 Magnetic domains and magnetic domain walls. Ph.D. thesis, Courant Institute of Mathematical Sciences, New York University.

García-Cervera, C. J. 2004 One-dimensional magnetic domain walls. *Eur. J. Appl. Math.* **15**, 451–486.

García-Cervera, C. J. In press. Néel walls in low anisotropy double layers. *SIAM J. Appl. Math.*

Hirota, E., Sakakima, H. & Inomata, K. 2002 *Giant magneto-resistance devices.* Berlin: Springer.

Hubert, A. & Schäfer, R. 1998 *Magnetic domains: the analysis of magnetic microstructures.* Berlin: Springer.

Isaacson, E. & Keller, H. B. 1966 *Analysis of numerical methods.* New York: Wiley.

Landau, L. & Lifshitz, E. 1935 On the theory of the dispersion of magnetic permeability in ferromagnetic bodies. *Phys. Z. Sowjetunion* **8**, 153–169.

Melcher, C. 2003 The logarithmic tail of Néel walls. *Arch. Ration. Mech. Anal.*, 168.

Melcher, C. 2004 Logarithmic lower bounds for Néel walls. *Calc. Var. PDE* **21**, 209–219.

Middelhoek, S. 1966 Domain wall structures in magnetic double films. *J. Appl. Phys.* **37**, 1276–1282.

Nocedal, J. & Wright, S. J. 1999 *Numerical optimization.* Springer Series in Operations Research. New York: Springer.

Otto, F. 2002 Cross-over in scaling laws: a simple example from micromagnetics. In *Proceedings of the International Congress of Mathematicians, Beijing*, vol. III, pp. 829–838. Beijing: Higher Ed. Press.

Prinz, G. 1998 Magnetoelectronics. *Science* **282**, 1660.

Puchalska, I. B. & Niedoba, H. 1991 Magnetization process in permalloy multilayer films. *IEEE Trans. Magn.* **27**, 3579–3587.

Slonczewski, J. C. 1966 Theory of domain-wall structure in multiple magnetic films. *IBM J. Res. Dev.* **10**, 377–387.

Slonczewski, J. C. 1966 Structure of domain walls in multiple films. *J. Appl. Phys.* **37**, 1268–1269.

Ziese, M. & Thornton, M. J. (eds) 2001. *Spin electronics.* Springer Lecture Notes in Physics, vol. 569. Berlin: Springer.